Scattering from a Domain Wall
in a Spontaneously Broken Gauge Theory

Glennys R. Farrar[1]

Department of Physics and Astronomy

Rutgers University, Piscataway, NJ 08855, USA

John W. McIntosh, Jr.

Physics Department

Princeton University, Princeton, NJ 08544, USA

Abstract: We study the interaction of particles with a domain wall at a symmetry-breaking phase transition by perturbing about the domain wall solution. We find the particulate excitations appropriate near the domain wall and relate them to the particles present far from the wall in the uniform broken and unbroken phases. For a quartic Higgs potential we find analytic solutions to the equations of motion and derive reflection and transmission coefficients. We discover several bound states for particles near the wall. Finally, we apply our results to the electroweak phase transition in the standard model.

Contents

1　Introduction

During a first-order phase transition in which a gauge symmetry is spontaneously broken, a number of effects depend on the scattering of particles from the domain wall between the phases of broken and unbroken symmetry. For instance, at the electroweak phase transition, a difference in the reflection coefficients of particles carrying opposite quantum numbers could play a role in producing the baryon asymmetry of the universe. Analytic solutions for quark scattering from domain walls of two different profiles are already in the literature [1, 2], but so far there has been no analogous treatment for the bosons of the theory. The study of boson scattering at a symmetry-breaking phase transition is complicated by the fact that the two phases have different particle contents, as explained by the Higgs mechanism. Addressing this difficulty is the main focus of the present work.

We begin by considering the simplest gauge theory with spontaneous symmetry breaking, the Abelian Higgs model. To permit a static domain wall to exist, we study the theory at its transition temperature. We find the modes of particulate excitation appropriate near the domain wall and express the interaction of these modes with the wall in terms of a one-dimensional scattering potential. We relate these internal modes to the particle modes present in the asymptotic broken and unbroken phases. All these results are valid for a general Higgs potential.

In section 3 we specialize to a quartic Higgs potential and obtain analytic solutions to the one-dimensional scattering equations for the internal modes, including solutions which describe bound states. Using the connections between internal and asymptotic modes derived in section 2 we compute scattering probabilities for the asymptotic particle states.

Having completed our analysis of the Abelian Higgs model, we proceed in section 4 to study the electroweak phase transition in the standard model. As a nonabelian gauge theory with partial symmetry breaking, the standard

1

model should be representative of the entire class of spontaneously broken gauge theories. We find that our results for the Abelian Higgs model may be adapted without difficulty to the case of the bosons in the standard model. We complete our discussion of the standard model by applying the methods of the previous sections to the case of the fermions. Specifically, we obtain internal and asymptotic modes, scattering potentials, and connection matrices for fermion scattering.

2 Internal and asymptotic modes

2.1 The model

The Abelian Higgs model contains two fields, a complex scalar field ϕ and a $U(1)$ gauge field A^μ. The Lagrangian is

$$\mathcal{L} = -\frac{1}{4}F_{\mu\nu}F^{\mu\nu} + (D_\mu\phi)^*(D^\mu\phi) - V(\sqrt{2}\,|\phi|). \tag{1}$$

The covariant derivative

$$D_\mu = \partial_\mu + ieA_\mu \tag{2}$$

gives ϕ a charge $+e$. We place only a few conditions on the Higgs potential V. There must be a minimum at zero for the unbroken-symmetry phase, and another minimum at some v_0 for the broken phase. For a stable domain wall to exist we need $V(v_0) = V(0)$; for convenience we take the common value to be zero.

We expand the field ϕ into real and imaginary parts as

$$\phi = \frac{1}{\sqrt{2}}(\phi_1 + i\phi_2). \tag{3}$$

The Lagrangian becomes

$$\mathcal{L} = -\frac{1}{4}F_{\mu\nu}F^{\mu\nu} + \frac{1}{2}(\partial_\mu\phi_1 - eA_\mu\phi_2)^2 + \frac{1}{2}(\partial_\mu\phi_2 + eA_\mu\phi_1)^2 - V(\sqrt{\phi_1^2 + \phi_2^2}). \tag{4}$$

Minimizing the action gives equations of motion for the three fields ϕ_1, ϕ_2 and A^μ:

$$\Box\phi_1 = e\phi_2 \partial \cdot A + 2eA^\mu \partial_\mu \phi_2 + e^2 A^2 \phi_1 - V'(\sqrt{\phi_1^2 + \phi_2^2})\frac{\phi_1}{\sqrt{\phi_1^2 + \phi_2^2}} \quad (5)$$

$$\Box\phi_2 = -e\phi_1 \partial \cdot A - 2eA^\mu \partial_\mu \phi_1 + e^2 A^2 \phi_2 - V'(\sqrt{\phi_1^2 + \phi_2^2})\frac{\phi_2}{\sqrt{\phi_1^2 + \phi_2^2}} \quad (6)$$

$$\partial_\nu F^{\mu\nu} = e(\phi_1 \partial^\mu \phi_2 - \phi_2 \partial^\mu \phi_1) + e^2 A^\mu (\phi_1^2 + \phi_2^2). \quad (7)$$

These equations of motion have a stable domain wall solution with $\phi_1 = v(z)$ and $\phi_2 = A^\mu = 0$. We will find this solution and study small perturbations about it. We write

$$\phi_1 = v(z) + h \quad (8)$$

and take h, ϕ_2 and A^μ to be perturbatively small.

The term of order zero in equation (5) is the condition for the field configuration $v(z)$ to be stable:

$$v'' = V'(v). \quad (9)$$

We allow the prime symbol to have two meanings: since V is a function of v we take V' to be dV/dv; in all other cases a prime indicates a derivative with respect to z. Integrating equation (9) twice gives the domain wall solution

$$z = \int_{v_0/2}^{v(z)} \frac{d\tilde{v}}{\sqrt{2V(\tilde{v})}} \quad (10)$$

in which the unbroken phase is taken to be at $z = -\infty$. We will also make use of the solutions $v = v_0$ and $v = 0$ which describe uniform broken and unbroken phases.

The first-order terms in equations (5)–(7) consist of an equation for the field h

$$\Box h = -V''(v)h \quad (11)$$

3

and the following coupled equations for ϕ_2 and A^μ:

$$\Box\phi_2 = -ev\,\partial \cdot A - 2eA^\mu\partial_\mu v - \frac{V'(v)}{v}\phi_2 \qquad (12)$$

$$\partial_\nu F^{\mu\nu} = e(v\partial^\mu\phi_2 - \phi_2\partial^\mu v) + (ev)^2 A^\mu. \qquad (13)$$

If we take the divergence of equation (13) and apply the condition (9) on the background field we get equation (12) times a factor ev. Thus equation (12) is redundant as long as v is not zero.

2.2 Particle content far from the wall

To obtain the first-order equations appropriate to the phase of unbroken symmetry we set $v = 0$ in equations (11)–(13). Equation (11) for h becomes

$$(\Box + m^2)h = 0, \qquad (14)$$

where the mass m is defined by

$$m^2 = V''(0). \qquad (15)$$

Since v is zero, equation (12) is not redundant; it reduces to

$$(\Box + m^2)\phi_2 = 0. \qquad (16)$$

Equations (14) and (16) combine to give a single Klein-Gordon equation for the complex field ϕ:

$$(\Box + m^2)\phi = 0. \qquad (17)$$

The final first-order equation (13) simplifies to

$$\partial_\nu F^{\mu\nu} = 0. \qquad (18)$$

These perturbative equations tell us that the unbroken phase contains a complex scalar field ϕ of mass m and a massless vector boson A^μ. Our

linearized equations of motion describe only the interaction of particles with the background field v, not the interaction of particles with each other, so we must refer back to the original Lagrangian to find out that the scalar field ϕ carries charge $+e$.

We define the following normalized solutions of equations (17) and (18). Their meaning and use are discussed below.

$$
\begin{array}{c|rcl}
\phi^+ & \phi & = & \frac{1}{2}\mathrm{e}^{-ip\cdot x} \\
\phi^- & \phi & = & \frac{1}{2}\mathrm{e}^{ip\cdot x} \\
A_T & A^\mu & = & \varepsilon^\mu \mathrm{e}^{-ip\cdot x}
\end{array}
\tag{19}
$$

We choose our coordinate system so that the four-vector p^μ is $(\omega, p, 0, k)$. The energy ω is always positive, but the momenta p and k may have either sign. The solutions (19) are normalized so that their time-averaged z-component of energy flux is $\frac{1}{2}\omega k$. In the case of the gauge boson solution A_T the normalization assumes that the polarization vector ε^μ satisfies

$$
\varepsilon^2 = -1.
\tag{20}
$$

Although we use complex notation, the field A^μ is real-valued; the operation of taking the real part is implied. We subdivide A_T into two polarizations A_{T1} and A_{T2} with polarization vectors

$$
\varepsilon_{T1} = (0, k, 0, -p)/\sqrt{p^2 + k^2}
\tag{21}
$$

$$
\varepsilon_{T2} = (0, 0, 1, 0).
\tag{22}
$$

Using these standard solutions we can describe a field configuration with a single complex number. For example, the complex number A_{T1} represents the solution

$$
A^\mu = A_{T1}\, \varepsilon_{T1}^\mu \mathrm{e}^{-ip\cdot x}.
\tag{23}
$$

When a standard solution has negative energy we define the coefficient of the solution to be the complex conjugate of the given complex number. For

example, the complex number ϕ^- represents the solution

$$\phi = (\phi^-)^* \tfrac{1}{2} e^{ip \cdot x}. \tag{24}$$

Next we consider the phase of broken symmetry. Setting $v = v_0$ we find that the first-order equations (11)–(13) reduce to

$$(\Box + \tilde{m}^2)h = 0 \tag{25}$$
$$\partial_\nu F^{\mu\nu} = ev_0 \partial^\mu \phi_2 + (ev_0)^2 A^\mu, \tag{26}$$

where

$$\tilde{m}^2 = V''(v_0). \tag{27}$$

Defining the variable

$$B^\mu = A^\mu + \partial^\mu \left(\frac{\phi_2}{ev}\right) \tag{28}$$

which is invariant under perturbatively small gauge transformations allows us to simplify equation (26) to

$$\partial_\nu F_B^{\mu\nu} = M^2 B^\mu, \tag{29}$$

where the mass M is given by

$$M^2 = (ev_0)^2. \tag{30}$$

According to equations (25) and (29) the broken phase contains a Higgs scalar h of mass $\tilde{m}$ and a massive vector boson B^μ of mass M.

The normalized solutions of the broken-phase equations are as follows:

$$\begin{array}{c|cc} h & h & = & e^{-ip \cdot x} \\ \hline B & B^\mu & = & \varepsilon^\mu e^{-ip \cdot x} \end{array} \tag{31}$$

In addition to transverse modes B_{T1} and B_{T2} with the polarizations ε_{T1} and ε_{T2} given above, the massive vector boson has a longitudinal mode B_L with polarization

$$\varepsilon_L = \left(\frac{\omega}{M\sqrt{\omega^2 - M^2}}\right)\left(\frac{\omega^2 - M^2}{\omega}, p, 0, k\right). \tag{32}$$

2.3 Separation of scalar internal modes

We will reduce the equations of motion (11)–(13) in the domain wall background to independent scalar equations of the form

$$\left[\Box + U(z)\right] S = 0, \tag{33}$$

where S is a scalar mode and U is the potential it sees. We take all fields to be eigenstates of energy and transverse momentum, that is, to contain a factor $e^{-i\omega t + ipx}$. Once we define the positive quantity E by

$$E^2 = \omega^2 - p^2, \tag{34}$$

equation (33) becomes the Schrödinger equation

$$\left[-\partial_3^2 + U(z)\right] S = E^2 S \tag{35}$$

for a particle with nonrelativistic energy E^2, so our intuition for one-dimensional scattering can be applied to the potential U. Equation (33) shows that the asymptotic values $U(\pm\infty)$ are to be identified with the mass squared of the scalar mode in the broken and unbroken phases.

Equation (11) for h is already in the required scalar form—we need only define the potential

$$U_h(z) = V''(v(z)). \tag{36}$$

To extract scalar modes from equation (13) for A^μ, the first thing we do is write the equation in terms of the variable B^μ (28):

$$\partial_\nu F_B^{\mu\nu} = (ev)^2 B^\mu. \tag{37}$$

We can get two scalar modes by making the ansatz $B^3 = 0$. In this case, taking the divergence of equation (37) produces the relation $\partial \cdot B = 0$, which allows us to simplify equation (37) to

$$-\Box B^\mu = (ev)^2 B^\mu. \tag{38}$$

Factoring out a constant polarization by writing

$$B^\mu = \varepsilon^\mu \tau \tag{39}$$

gives a scalar equation for τ, with potential

$$U_\tau = (ev)^2. \tag{40}$$

The constraints on B^μ allow two polarizations:

$$\varepsilon_{\tau 1} = (p, \omega, 0, 0)/E \tag{41}$$

$$\varepsilon_{\tau 2} = (0, 0, 1, 0). \tag{42}$$

We name the two corresponding scalar modes $B_{\tau 1}$ and $B_{\tau 2}$.

To obtain a third scalar mode from equation (37) we make the reasonable assumption that the polarization of the third mode is orthogonal to the polarizations of the two we already have. Referring back to equations (41) and (42) we find that orthogonality requires the first three components of the polarization of the third mode to be proportional to $(\omega, p, 0)$, so we can write

$$B^\mu = \partial^\mu b \qquad \text{for } \mu \neq 3. \tag{43}$$

Now the four components of equation (37) reduce to the following two equations:

$$[-\partial_3^2 + (ev)^2]\, b = \partial_3 B^3 \tag{44}$$

$$[-E^2 + (ev)^2]B^3 = E^2 \partial_3 b. \tag{45}$$

Solving for b in terms of B^3 yields[2]

$$b = \frac{1}{E^2(ev)^2}\partial_3[(ev)^2 B^3]; \tag{46}$$

---

[2]We must eliminate b rather than B^3, for the following heuristic reason: Suppose we send a particle with the third polarization toward the wall with energy low enough that it will be totally reflected. When the particle reaches the classical turning point its momentum is $(\omega, p, 0, 0)$. Now, for a massive vector boson with this momentum the third polarization is $(0, 0, 0, 1)$, so at this particular point in the scattering b will be forced to zero, not by the differential equation it obeys, but by the changing polarization vector. B^3 has no such singularity.
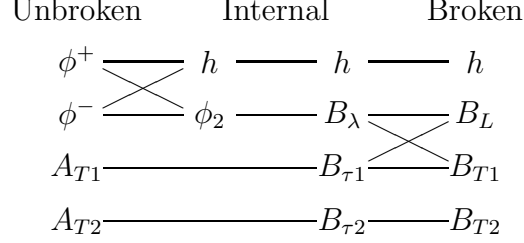
Unbroken   Internal   Broken

ϕ^+ —✕— h —— h —— h

ϕ^- —✕— ϕ_2 —— B_λ —✕— B_L

A_{T1} ——————— $B_{\tau1}$ —✕— B_{T1}

A_{T2} ——————— $B_{\tau2}$ —— B_{T2}

Figure 1: Connections between internal and asymptotic modes.

the remaining equation of motion is

$$\left[-E^2 - \partial_3^2 - 2\left(\frac{v'}{v}\right)\partial_3 + (ev)^2 + 2\left(\frac{v'}{v}\right)^2 - 2\frac{v''}{v}\right]B^3 = 0. \tag{47}$$

Defining

$$B^3 = (E/ev)\lambda \tag{48}$$

removes the linear derivative term, leaving

$$\left[-E^2 - \partial_3^2 + (ev)^2 + 2\left(\frac{v'}{v}\right)^2 - \frac{v''}{v}\right]\lambda = 0, \tag{49}$$

a scalar scattering equation with potential

$$U_\lambda = (ev)^2 + 2\left(\frac{v'}{v}\right)^2 - \frac{v''}{v}. \tag{50}$$

This scalar mode, which describes the third polarization of the field B^μ, we refer to by the name B_λ.

2.4 Connection of internal and asymptotic modes

A schematic diagram of how the various modes connect to one another is given in figure 1. We will devote the rest of this section to making a precise statement of what this diagram means.

The fields h and B^μ which describe the scattering process are the same as the fields in the broken phase, so to find the connection between modes

p^μ	ω	p	0	k	
ε_L	$\frac{\omega^2-M^2}{\omega}$	p	0	k	$\frac{\omega}{M\sqrt{\omega^2-M^2}}$
ε_{T1}	0	k	0	$-p$	$\frac{1}{\sqrt{p^2+k^2}}$
ε_{T2}	0	0	1	0	
ε_λ	ω	p	0	$\frac{E^2}{k}$	$\frac{k}{ME}$
$\varepsilon_{\tau 1}$	p	ω	0	0	$\frac{1}{E}$
$\varepsilon_{\tau 2}$	0	0	1	0	

Table 1: Summary of polarization vectors. The vector ε_λ is only meaningful in the broken phase. The last column contains normalization factors for the normalization $\varepsilon^2 = -1$.

at $+\infty$ we need only express the asymptotic polarizations of B^μ in terms of the internal ones. We summarize the various polarization vectors in table 1. The only new information in this table is the polarization vector ε_λ. To calculate this vector, we consider a scalar function λ which is asymptotically a plane wave:

$$\lambda = \mathrm{e}^{-ip\cdot x}. \tag{51}$$

Working backward through equations (48), (46), and (43) we find

$$B^3 = \left(\frac{E}{ev}\right)\mathrm{e}^{-ip\cdot x} \tag{52}$$

$$b = \frac{1}{E(ev)}\left(ik + \frac{v'}{v}\right)\mathrm{e}^{-ip\cdot x} \tag{53}$$

$$B^\mu = \frac{p^\mu}{E(ev)}\left(k - i\frac{v'}{v}\right)\mathrm{e}^{-ip\cdot x}. \tag{54}$$

Using the fact that $v'/v \to 0$ in the broken phase, we read off the unnormalized polarization vector from equations (52) and (54).

Expanding the broken-phase polarization vectors in terms of the internal ones we obtain the following matrix equation connecting the internal modes

10

to the broken-phase modes:

$$
\begin{pmatrix} h \\ B_L \\ B_{T1} \\ B_{T2} \end{pmatrix}
=
\begin{pmatrix}
1 & & & \\
 & \dfrac{\omega k}{E\sqrt{p^2+k^2}} & \dfrac{pM}{E\sqrt{p^2+k^2}} & \\
 & -\dfrac{pM}{E\sqrt{p^2+k^2}} & \dfrac{\omega k}{E\sqrt{p^2+k^2}} & \\
 & & & 1
\end{pmatrix}
\begin{pmatrix} h \\ B_\lambda \\ B_{\tau 1} \\ B_{\tau 2} \end{pmatrix},
\tag{55}
$$

where zeroes in the matrix have been replaced by blanks for legibility. At normal incidence the matrix reduces to the identity.

The connection between the internal modes and the asymptotic modes in the unbroken phase is more involved. We begin with the simplest case, the connection between $B_{\tau 2}$ and A_{T2}. We consider a solution of the scattering equation for the $B_{\tau 2}$ mode which is asymptotically a plane wave, that is, for which there is a complex number $B_{\tau 2}$ such that

$$
\tau - B_{\tau 2}\mathrm{e}^{-ip\cdot x} \to 0 \qquad \text{as} \qquad z \to -\infty.
\tag{56}
$$

According to the definition (39) of τ, this solution generates a field configuration

$$
B^\mu[B_{\tau 2}] = \varepsilon_{\tau 2}^\mu \tau.
\tag{57}
$$

On the other hand, from the definition (28) of B^μ we find that the field configuration generated by the standard solution for the A_{T2} mode is

$$
B^\mu[A_{T2}] = A_{T2}\,\varepsilon_{T2}^\mu \mathrm{e}^{-ip\cdot x}.
\tag{58}
$$

If we take A_{T2} equal to $B_{\tau 2}$, the two field configurations are asymptotically the same, that is,

$$
B^\mu[B_{\tau 2}] - B^\mu[A_{T2}] \to 0 \qquad \text{as} \qquad z \to -\infty.
\tag{59}
$$

We use this condition—that the difference between field configurations go to zero—as our criterion for connection.

11

We handle the $B_{\tau 1}$ mode similarly. An internal solution with asymptotic form

$$\tau = B_{\tau 1}\mathrm{e}^{-ip\cdot x} \tag{60}$$

generates an asymptotic field configuration

$$B^{\mu}[B_{\tau 1}] = B_{\tau 1}\,\varepsilon^{\mu}_{\tau 1}\mathrm{e}^{-ip\cdot x}. \tag{61}$$

Applying the relation

$$\varepsilon^{\mu}_{\tau 1} = (\mathrm{sgn}\,k)\,\varepsilon^{\mu}_{T1} + \left(\frac{p}{\omega E}\right)p^{\mu} \tag{62}$$

separates $B^{\mu}[B_{\tau 1}]$ into two terms. The first term matches the field $B^{\mu}[A_{T1}]$ generated by an A_{T1} solution with amplitude $A_{T1} = (\mathrm{sgn}\,k)B_{\tau 1}$. The second term describes a field

$$A^{\mu} = B_{\tau 1}\left(\frac{p}{\omega E}\right)p^{\mu}\mathrm{e}^{-ip\cdot x} \tag{63}$$

polarized in the direction of p^{μ}. Although the field (63) is a valid solution of the unbroken-phase equation of motion (18) for A^{μ}, it has a field strength ($F^{\mu\nu}$) of zero and so carries no energy or momentum. We discard this pure gauge solution and find that $B_{\tau 1}$ connects directly to A_{T1}.

The use of the coefficients $B_{\tau 1}$ and $B_{\tau 2}$ in the preceding paragraphs has obeyed the following convention, which we will continue to observe: whenever we use a complex number to describe the asymptotic form of one of the internal modes, the number is the coefficient of a unit-amplitude plane wave. We will apply the same convention to h and ϕ_2 even though they are not internal modes.

Next we discuss the connection between the internal mode B_{λ} and the asymptotic modes in the unbroken phase. A solution of the scattering equation which is asymptotically a plane wave, that is, for which

$$\lambda - B_{\lambda}\mathrm{e}^{-ip\cdot x} \to 0 \qquad \mathrm{as} \qquad z \to -\infty, \tag{64}$$

12

generates an asymptotic field configuration

$$B^3[B_\lambda] = B_\lambda\left(\frac{E}{ev}\right)\mathrm{e}^{-ip\cdot x}. \tag{65}$$

Since $v \to 0$ in the unbroken phase, this field configuration is divergent. However, we can obtain an equal divergence from the asymptotic field ϕ_2. We take ϕ_2 to be a plane wave with amplitude given by the complex number ϕ_2 and substitute into the definition (28) of B^μ to find

$$B^3[\phi_2] = \phi_2\left(\frac{1}{ev}\right)\left(\frac{v'}{v} - ik\right)\mathrm{e}^{-ip\cdot x}. \tag{66}$$

As $v \to 0$, the ratio v'/v reduces to m, so we can match the two divergences by taking

$$\phi_2 = \frac{E}{m-ik}B_\lambda = \frac{m+ik}{E}B_\lambda. \tag{67}$$

Although equation (67) will turn out to be the correct relation between the modes B_λ and ϕ_2, the above argument using matching divergences does not prove that the two modes connect, because the difference of the matching divergences contains a finite part which does not necessarily go to zero as $z \to -\infty$. To calculate the finite part of the field $B^\mu[B_\lambda]$ correctly, we keep the first-order term in the asymptotic expansion of λ near $v = 0$, writing

$$\lambda = B_\lambda(1 + cv)\mathrm{e}^{-ip\cdot x}, \tag{68}$$

where the constant c is determined by the scattering equation (49) for the B_λ mode. A calculation which we omit shows that when the relation between the modes B_λ and ϕ_2 is that given in equation (67), the field configurations $B^\mu[B_\lambda]$ and $B^\mu[\phi_2]$ satisfy

$$B^\mu[B_\lambda] - \left(B^\mu[\phi_2] + C\,p^\mu\mathrm{e}^{-ip\cdot x}\right) \to 0 \qquad \text{as} \qquad z \to 0, \tag{69}$$

where the coefficient C of the pure gauge solution is an appropriately chosen constant. In other words, the field configuration $B^\mu[B_\lambda]$ is asymptotically

13

equal to the field $B^\mu[\phi_2]$ plus a pure gauge term. We discard the pure gauge solution and find that B_λ connects to ϕ_2 as in equation (67).

All that remains is to combine the ϕ_2 produced by B_λ with the internal mode h to get the unbroken-phase modes ϕ^+ and ϕ^-. Since h and ϕ_2 are real-valued fields, the amplitudes h and ϕ_2 actually represent the functions

$$\frac{h}{2}\mathrm{e}^{-ip\cdot x} + \frac{h^*}{2}\mathrm{e}^{ip\cdot x} \tag{70}$$

and

$$\frac{\phi_2}{2}\mathrm{e}^{-ip\cdot x} + \frac{\phi_2^*}{2}\mathrm{e}^{ip\cdot x} \tag{71}$$

which we combine into

$$\phi[h, \phi_2] = \left(\frac{h + i\phi_2}{\sqrt{2}}\right)\left(\frac{1}{2}\mathrm{e}^{-ip\cdot x}\right) + \left(\frac{h^* + i\phi_2^*}{\sqrt{2}}\right)\left(\frac{1}{2}\mathrm{e}^{ip\cdot x}\right). \tag{72}$$

Using the normalized solutions (19) we read off the amplitudes

$$\phi^+ = \frac{h + i\phi_2}{\sqrt{2}} \qquad \text{and} \qquad \phi^- = \frac{h - i\phi_2}{\sqrt{2}}. \tag{73}$$

We collect all our results about the connection between the internal and unbroken-phase modes in the following equation:

$$\begin{pmatrix} \phi^+ \\ \phi^- \\ A_{T1} \\ A_{T2} \end{pmatrix} = \begin{pmatrix} 1/\sqrt{2} & -\frac{k-im}{E\sqrt{2}} & & \\ 1/\sqrt{2} & \frac{k-im}{E\sqrt{2}} & & \\ & & \operatorname{sgn} k & \\ & & & 1 \end{pmatrix} \begin{pmatrix} h \\ B_\lambda \\ B_{\tau 1} \\ B_{\tau 2} \end{pmatrix}. \tag{74}$$

The matrix equations (55) and (74) are the desired precise statement of what the connection diagram in figure 1 means.

3   Scattering from the domain wall

3.1   Specification of the potential

All our results up to this point are independent of the details of the Higgs potential $V(v)$. To obtain anything more than generalities about scattering

14

from the domain wall, however, it is necessary to give up this independence and specify a form for the potential. We choose the standard quartic potential

$$V(v) = \frac{1}{4}\lambda v^2(v - v_0)^2. \tag{75}$$

In section 3.7 we will discuss how our results depend on this choice.

With this choice of potential the mass m (15) of the charged scalars is equal to the mass $\widetilde{m}$ (27) of the Higgs,

$$m^2 = \widetilde{m}^2 = \frac{1}{2}\lambda v_0^2, \tag{76}$$

and the integral (10) which determines the background field can be evaluated explicitly, with result

$$v(z) = \frac{v_0}{2}\left(1 + \tanh\frac{mz}{2}\right). \tag{77}$$

The scattering potentials U_h, U_τ and U_λ can be cast into the standard form

$$U = m^2\Big[U_0(1 - s) + U_1 s + U_2 s(1 - s)\Big], \tag{78}$$

where the dimensionless coordinate s is defined by

$$s = \frac{1}{2}\left(1 + \tanh\frac{mz}{2}\right) = \frac{v}{v_0}. \tag{79}$$

The coefficients U_0, U_1 and U_2 for the various potentials are listed in table 2.

3.2 Solution using hypergeometric functions

In this section we solve the scattering equation

$$[\Box + U(z)]\, S = 0 \tag{33}$$

analytically for any potential U of the standard form (78), that is, any potential quadratic in the variable s. Although our results are more general,

15

	General V	Specific V	U_0	U_1	U_2
h	$U_h = V''(v)$	$m^2[1 - 6s(1 - s)]$	1	1	-6
B_τ	$U_\tau = (ev)^2$	$M^2 s^2$	0	$\mathcal{M}^2$	$-\mathcal{M}^2$
B_λ	$U_\lambda = (ev)^2 + 2(\frac{v'}{v})^2 - \frac{v''}{v}$	$m^2(1 - s) + M^2 s^2$	1	$\mathcal{M}^2$	$-\mathcal{M}^2$

Table 2: Summary of internal mode scattering potentials. The mass ratio $\mathcal{M}^2$ is defined to be M^2/m^2.

our method of solution is similar to that used by Ayala et al [2] to study the scattering of fermions. We factor S into

$$S = s^{\kappa_0}(1 - s)^{\kappa_1} \tilde{S}(s)\, e^{-i\omega t + ipx}, \tag{80}$$

where κ_0 and κ_1 are constants to be determined, and find that the scattering equation becomes

$$
\begin{aligned}
\Big[s^2(1 - s)^2 \frac{d^2}{ds^2} & \\
+ \ \Big(2\kappa_0\, s(1 - s)^2 &- 2\kappa_1\, s^2(1 - s) + s(1 - s)(1 - 2s) \Big)\frac{d}{ds} \\
+ \ \Big(\kappa_0{}^2\,(1 - s)^2 &+ \kappa_1{}^2\, s^2 - (\kappa_0 + \kappa_1 + 2\kappa_0\kappa_1)\, s(1 - s) \\
&+ \frac{E^2}{m^2} - U_0\,(1 - s) - U_1\, s - U_2\, s(1 - s) \Big) \Big]\, \tilde{S} = 0.
\end{aligned} \tag{81}
$$

Setting

$$\kappa_i{}^2 = U_i - \frac{E^2}{m^2} \tag{82}$$

makes equation (81) divisible by $s(1 - s)$; the quotient is the hypergeometric equation[3]

$$\Big[s(1 - s)\frac{d^2}{ds^2} + \Big(\gamma - (\alpha + \beta + 1)s \Big)\frac{d}{ds} - \alpha\beta \Big]\tilde{S} = 0 \tag{83}$$

[3]All the relevant facts about the hypergeometric equation appear in reference [3].

16

with parameters

$$
\begin{aligned}
\alpha &= \kappa_0 + \kappa_1 + \tfrac{1}{2} + \delta \\
\beta &= \kappa_0 + \kappa_1 + \tfrac{1}{2} - \delta \\
\gamma &= 1 + 2\kappa_0.
\end{aligned}
\tag{84}
$$

The constant δ is defined by

$$
\delta = \sqrt{1/4 - U_2}.
\tag{85}
$$

One solution of the hypergeometric equation (83) is the hypergeometric function $F(\alpha, \beta, \gamma; s)$, and the corresponding solution of the scattering equation (33) is

$$
S = s^{\kappa_0}(1-s)^{\kappa_1} F(\alpha, \beta, \gamma; s)\, e^{-i\omega t + ipx}.
\tag{86}
$$

We study the asymptotic behavior of this solution, beginning with the case $z \to -\infty$, that is, $s \to 0$. As its argument s goes to zero the function F reduces to unity, as does the factor $(1-s)^{\kappa_1}$. From equation (79) we find that as $z \to -\infty$ the coordinate s simplifies to e^{mz}, so the solution (86) is asymptotically the plane wave

$$
e^{-i\omega t + ipx + m\kappa_0 z}.
\tag{87}
$$

For the solution to describe scattering, this exponential must represent the transmitted part of a wave incident from $z = +\infty$, that is, κ_0 must be negative imaginary. To avoid confusion, we take κ_1 to be negative imaginary as well.

To calculate the asymptotic behavior of the solution (86) in the opposite limit $z \to +\infty$ we use the identity

$$
F(\alpha, \beta, \gamma; s) = \frac{\Gamma(\gamma)\Gamma(\gamma - \alpha - \beta)}{\Gamma(\gamma - \alpha)\Gamma(\gamma - \beta)} F(\alpha, \beta, \alpha + \beta + 1 - \gamma; 1 - s)
\tag{88}
$$

$$
+ \frac{\Gamma(\gamma)\Gamma(\alpha + \beta - \gamma)}{\Gamma(\alpha)\Gamma(\beta)} (1-s)^{\gamma - \alpha - \beta} F(\gamma - \alpha, \gamma - \beta, \gamma + 1 - \alpha - \beta; 1 - s).
$$

17

Taking into account the parameter values (84) and replacing $1 - s$ by its equivalent e^{-mz} we find S has the following asymptotic form at $+\infty$:

$$\frac{\Gamma(1 + 2\kappa_0)\,\Gamma(-2\kappa_1)}{\Gamma(\kappa_0 - \kappa_1 + \frac{1}{2} + \delta)\,\Gamma(\kappa_0 - \kappa_1 + \frac{1}{2} - \delta)}\,\mathrm{e}^{-i\omega t + ipx - m\kappa_1 z}$$

$$+ \frac{\Gamma(1 + 2\kappa_0)\,\Gamma(2\kappa_1)}{\Gamma(\kappa_0 + \kappa_1 + \frac{1}{2} + \delta)\,\Gamma(\kappa_0 + \kappa_1 + \frac{1}{2} - \delta)}\,\mathrm{e}^{-i\omega t + ipx + m\kappa_1 z}. \qquad (89)$$

Since κ_1 is negative imaginary, the second term represents the incident wave. Taking the appropriate ratios yields the reflection and transmission coefficients

$$r = \frac{\Gamma(\kappa_0 + \kappa_1 + \frac{1}{2} + \delta)\,\Gamma(\kappa_0 + \kappa_1 + \frac{1}{2} - \delta)}{\Gamma(\kappa_0 - \kappa_1 + \frac{1}{2} + \delta)\,\Gamma(\kappa_0 - \kappa_1 + \frac{1}{2} - \delta)}\,\frac{\Gamma(-2\kappa_1)}{\Gamma(\ 2\kappa_1)} \qquad (90)$$

$$t = \frac{\Gamma(\kappa_0 + \kappa_1 + \frac{1}{2} + \delta)\,\Gamma(\kappa_0 + \kappa_1 + \frac{1}{2} - \delta)}{\Gamma(1 + 2\kappa_0)\,\Gamma(2\kappa_1)}. \qquad (91)$$

In the case of total reflection we make the transmitted wave (87) into a decaying exponential by taking κ_0 to be positive real. Although the particle is totally reflected, the transmission coefficient t does not become zero, and indeed it need not, being merely the coefficient of a decaying exponential. The reflection coefficient r does reach unit amplitude, however.

The solution of the hypergeometric equation (83) which represents a particle incident from $-\infty$ is

$$\tilde{S} = F(\alpha, \beta, \alpha + \beta + 1 - \gamma; 1 - s). \qquad (92)$$

Proceeding as before we find reflection and transmission coefficients which differ from the previous results (90) and (91) only by exchange of κ_0 and κ_1.

3.3 Bound states

To search for bound states we take both κ_0 and κ_1 to be positive real and require that the growing exponential in equation (89) have coefficient zero:

$$\frac{\Gamma(1 + 2\kappa_0)\,\Gamma(2\kappa_1)}{\Gamma(\kappa_0 + \kappa_1 + \frac{1}{2} + \delta)\,\Gamma(\kappa_0 + \kappa_1 + \frac{1}{2} - \delta)} = 0. \qquad (93)$$

The gamma function has no zeroes, but it does have a pole at each nonpositive integer. The parameter $\alpha = \kappa_0 + \kappa_1 + \frac{1}{2} + \delta$ is always either strictly positive or complex, so equation (93) reduces to the condition that the parameter $\beta = \kappa_0 + \kappa_1 + \frac{1}{2} - \delta$ be a nonpositive integer, that is, that

$$- \beta \equiv \delta - \tfrac{1}{2} - (\kappa_0 + \kappa_1) = n \tag{94}$$

for some nonnegative integer n. We attempt to satify this condition by varying the energy E^2. Our variations must keep κ_0 and κ_1 real-valued and strictly positive, which, according to the definition (82), means that

$$\frac{E^2}{m^2} < \min\left(U_0, U_1\right) \tag{95}$$

and therefore that

$$\kappa_0 + \kappa_1 > \sqrt{|U_0 - U_1|}. \tag{96}$$

As a result, $-\beta$ may take any value from $-\infty$ up to but not including a maximum N given by

$$N = \delta - \tfrac{1}{2} - \sqrt{|U_0 - U_1|}, \tag{97}$$

and equation (94) can be satisfied for any nonnegative integer $n < N$. Solving equation (94) for E^2 yields the energy of the corresponding bound state

$$\frac{E^2}{m^2} = \min\left(U_0, U_1\right) - \left(\frac{(\delta - \frac{1}{2} - n)^2 - |U_0 - U_1|}{2(\delta - \frac{1}{2} - n)}\right)^2. \tag{98}$$

For bound states the solution (86) of the hypergeometric equation simplifies, because when $-\beta$ is equal to a nonnegative integer n the power series for the hypergeometric function

$$F(\alpha, \beta, \gamma; s) = 1 + \frac{\alpha\beta}{\gamma}s + \frac{\alpha(\alpha+1)\beta(\beta+1)}{\gamma(\gamma+1)}\frac{s^2}{2!} + \cdots \tag{99}$$

collapses to a polynomial of degree n. The lowest-energy bound state has the particularly simple wavefunction

$$S = s^{\kappa_0}(1 - s)^{\kappa_1}\,\mathrm{e}^{-i\omega t + ipx}. \tag{100}$$

19

Using the parameters U_i given in table 2 we can compute the number of bound states for each of the internal modes. For the B_τ mode we find the bound state parameter N is never positive, so there are no bound states, but then we expect none in a potential without a minimum.

The h mode has $N = 2$ and so has two bound states. We apply equations (98)–(100) to find that the first bound state has energy $E^2 = 0$ and wavefunction

$$h = s(1-s)\,e^{-i\omega t+ipx} = \frac{1}{4}\,\text{sech}^2\,\frac{mz}{2}\,e^{-i\omega t+ipx} \qquad (101)$$

and that the second has energy $E^2 = (3/4)m^2$ and wavefunction

$$h = \sqrt{s(1-s)}\,(1-2s)\,e^{-i\omega t+ipx} = -\frac{1}{2}\,\text{sech}\,\frac{mz}{2}\,\tanh\frac{mz}{2}\,e^{-i\omega t+ipx}. \qquad (102)$$

To make a physical interpretation of these bound states we remember that h represents a small perturbation added to the background field v. The factor $\text{sech}^2(mz/2)$ which appears in the first bound state (101) is proportional to $v'(z)$, and adding a small amount of $v'(z)$ to v has the effect of translating the wall in the z-direction, so the wavefunction (101) describes a plane-wave oscillation of the local position of the wall. The second bound state (102) describes a similar oscillation of the local thickness of the wall. These two excitations of the wall can be thought of as quasiparticles confined to the wall surface with masses $\omega^2 - p^2 = E^2$ of zero and $(3/4)m^2$ respectively. No matter what Higgs potential V we choose, the h mode always has a bound state for oscillations of the wall position—we need only apply the equation of motion (9) for v to find that the wavefunction $h = v'(z)e^{-i\omega t+ipx}$ satisfies equation (11) whenever $E^2 = 0$. The underlying physical reason for the existence of this bound state is the translation invariance of the Lagrangian.

For mass ratios $\mathcal{M}^2 = M^2/m^2$ in the range $3/4 < \mathcal{M}^2 < 2$ the B_λ mode has a single bound state. Neither the energy (98) nor the wavefunction (100) of this state simplify further. The bound state parameter N and energy E^2 are plotted as functions of $\mathcal{M}^2$ in figure 2.
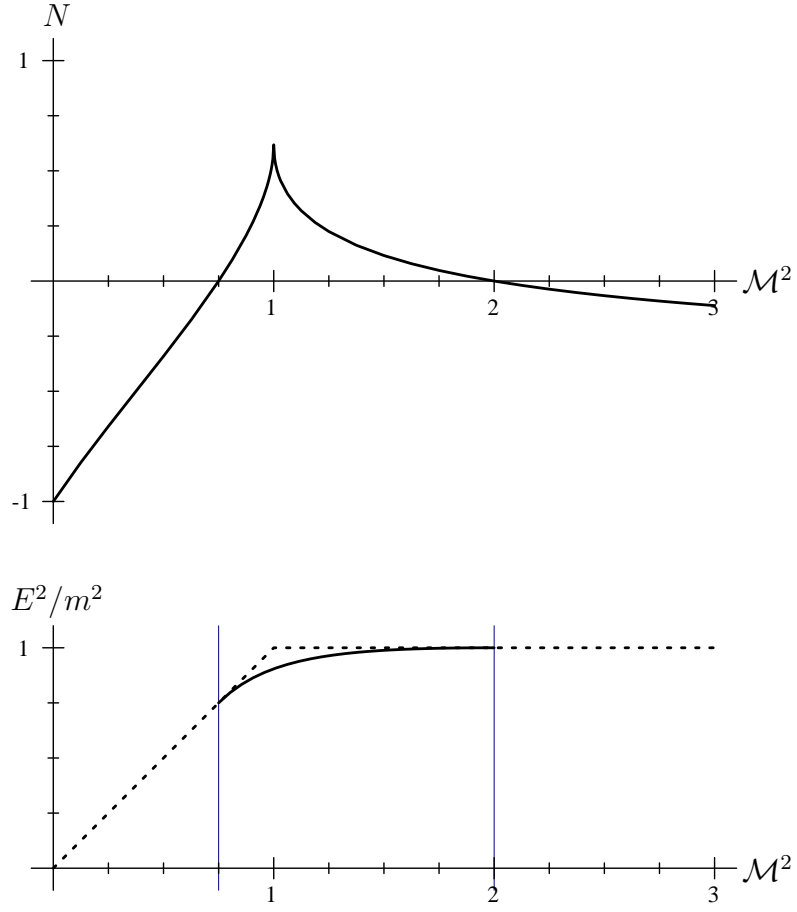
Figure 2: Bound state parameter N and bound state energy E^2/m^2 as functions of $\mathcal{M}^2$ for the B_λ mode. The dotted line in the second plot marks the start of the continuum of unbound states.

3.4 Reflection and transmission probabilities

For the case in which total reflection does not occur we calculate the reflection and transmission probabilities R and T for a particle incident from $+\infty$. Starting from the coefficients (90) and (91) and applying the identity

$$\Gamma(z)\Gamma(1-z) = \frac{\pi}{\sin \pi z} \tag{103}$$

we find

$$R = |r|^2 \;\; = \;\; \frac{\sin \pi(\kappa_0 - \kappa_1 + \frac{1}{2} + \delta)\sin \pi(\kappa_0 - \kappa_1 + \frac{1}{2} - \delta)}{\sin \pi(\kappa_0 + \kappa_1 + \frac{1}{2} + \delta)\sin \pi(\kappa_0 + \kappa_1 + \frac{1}{2} - \delta)} \tag{104}$$

$$T = \frac{k_0}{k_1}|t|^2 \;\; = \;\; \frac{-\sin 2\pi\kappa_0 \sin 2\pi\kappa_1}{\sin \pi(\kappa_0 + \kappa_1 + \frac{1}{2} + \delta)\sin \pi(\kappa_0 + \kappa_1 + \frac{1}{2} - \delta)} \tag{105}$$

where the asymptotic momenta k_i are given by

$$k_i = \sqrt{E^2 - m^2 U_i} = im\kappa_i. \tag{106}$$

The probabilities (104) and (105) are invariant under exchange of κ_0 and κ_1 and so apply to particles incident from $-\infty$ as well.

Using trigonometric identities we convert the transmission probability from equation (105) into the more practical form

$$T = \frac{2 \sinh \frac{2\pi k_0}{m} \sinh \frac{2\pi k_1}{m}}{\cosh \frac{2\pi k_0}{m} \cosh \frac{2\pi k_1}{m} + \sinh \frac{2\pi k_0}{m} \sinh \frac{2\pi k_1}{m} + \cos 2\pi\delta}. \tag{107}$$

Except in a few cases which we discuss momentarily, the transmission probability is a strictly increasing function of the energy E^2 with a square-root singularity at the threshold of total reflection. A typical curve is shown in figure 3. When $U_0 = U_1$ the square-root singularity is replaced by a linear approach to zero, unless also $\cos 2\pi\delta = -1$, in which case the transmission probability $T \equiv 1$ is no longer even strictly increasing. According to figure 3 the energy E^2 need only be a small fraction of the mass m^2 above threshold for the transmission probability to be significant. Other choices of the scattering
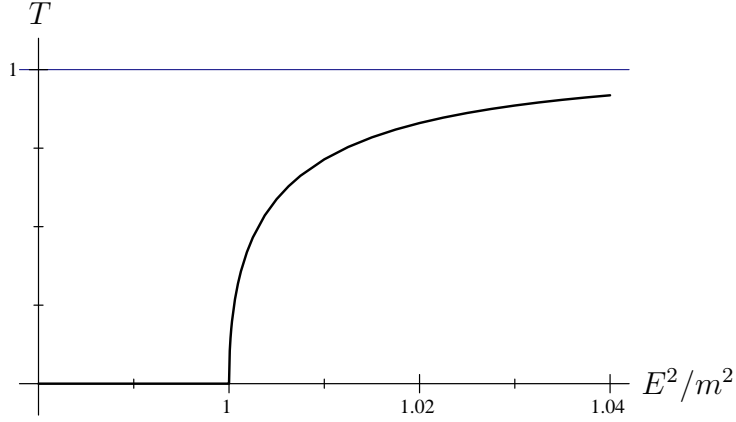
Figure 3: Transmission probability for the B_τ mode when $\mathcal{M}^2 = 1$.

potential do not make the onset of transmission significantly slower—in all cases the transmission probability reaches $1/2$ before E^2 gets $0.02\,m^2$ above the threshold. On the other hand, the onset becomes much faster as the potential approaches any of the potentials which give $T \equiv 1$.

The transmission curves for the B_τ and B_λ modes have the generic form described in the previous paragraph. If the gauge boson mass M were zero, the B_τ mode would have $T \equiv 1$, so if the gauge boson mass M is small compared to m the curve for the B_τ mode will have a sharp onset. The onset in the B_λ mode is never particularly sharp. For the h mode, $U_0 = U_1$ and $\delta = 5/2$ make the transmission probability *unity*. This result does not generalize to an arbitrary Higgs potential V. For most choices of V, the mass m of the charged scalars is different from the mass $\tilde{m}$ of the Higgs, so that reflection—in fact, total reflection—is possible.

3.5   Scattering of asymptotic modes

In section 2.4 we derived the connection equations

$$
\begin{pmatrix} h \\ B_L \\ B_{T1} \\ B_{T2} \end{pmatrix} = \begin{pmatrix} 1 & & & \\ & \frac{\omega k}{E\sqrt{p^2+k^2}} & \frac{pM}{E\sqrt{p^2+k^2}} & \\ & -\frac{pM}{E\sqrt{p^2+k^2}} & \frac{\omega k}{E\sqrt{p^2+k^2}} & \\ & & & 1 \end{pmatrix} \begin{pmatrix} h \\ B_\lambda \\ B_{\tau 1} \\ B_{\tau 2} \end{pmatrix} \tag{55}
$$

and

$$
\begin{pmatrix} \phi^+ \\ \phi^- \\ A_{T1} \\ A_{T2} \end{pmatrix} = \begin{pmatrix} 1/\sqrt{2} & -\frac{k-im}{E\sqrt{2}} & & \\ 1/\sqrt{2} & \frac{k-im}{E\sqrt{2}} & & \\ & & \operatorname{sgn} k & \\ & & & 1 \end{pmatrix} \begin{pmatrix} h \\ B_\lambda \\ B_{\tau 1} \\ B_{\tau 2} \end{pmatrix}. \tag{74}
$$

Using these two equations and the reflection and transmission coefficients (90) and (91) we can calculate scattering probabilities for a particle incident from the broken or unbroken phase. We use an inverted connection equation to convert a unit amplitude for the incident asymptotic mode into amplitudes for internal modes, multiply by the appropriate reflection and transmission coefficients to find the scattered amplitudes at both positive and negative infinity, and use the connection equations to convert back to amplitudes for asymptotic modes. We take the norm of these amplitudes to get probabilities, multiplying in the case of transmission by the appropriate momentum ratio.

The meaning of the symbol k depends on the context in which it appears. To avoid confusion, we define for each of the different particle masses a corresponding positive momentum, for example,

$$
k_m = \sqrt{E^2 - m^2}, \tag{108}
$$

and write each k in terms of these momenta. In the connection equation (55) for the broken phase, k is the momentum of a massive vector boson, that is, $|k| = k_M$. Because equation (55) expresses asymptotic amplitudes in the broken phase in terms of internal ones, we will apply it to particles moving

24

away from the wall, that is, particles with positive z-momentum. Setting $k = +k_M$ we obtain

$$
\begin{pmatrix} h \\ B_L \\ B_{T1} \\ B_{T2} \end{pmatrix} = \begin{pmatrix} 1 & & & \\ & \frac{\omega k_M}{E\sqrt{p^2+k_M^2}} & \frac{pM}{E\sqrt{p^2+k_M^2}} & \\ & -\frac{pM}{E\sqrt{p^2+k_M^2}} & \frac{\omega k_M}{E\sqrt{p^2+k_M^2}} & \\ & & & 1 \end{pmatrix} \begin{pmatrix} h \\ B_\lambda \\ B_{\tau 1} \\ B_{\tau 2} \end{pmatrix}.
\tag{109}
$$

To obtain the connection equation for particles moving toward the wall, we invert equation (55) and take $k = -k_M$, with result

$$
\begin{pmatrix} h \\ B_\lambda \\ B_{\tau 1} \\ B_{\tau 2} \end{pmatrix} = \begin{pmatrix} 1 & & & \\ & -\frac{\omega k_M}{E\sqrt{p^2+k_M^2}} & -\frac{pM}{E\sqrt{p^2+k_M^2}} & \\ & \frac{pM}{E\sqrt{p^2+k_M^2}} & -\frac{\omega k_M}{E\sqrt{p^2+k_M^2}} & \\ & & & 1 \end{pmatrix} \begin{pmatrix} h \\ B_L \\ B_{T1} \\ B_{T2} \end{pmatrix}.
\tag{110}
$$

Substituting $k = -k_m$ into equation (74) gives the connection equation for particles moving away from the wall into the unbroken phase,

$$
\begin{pmatrix} \phi^+ \\ \phi^- \\ A_{T1} \\ A_{T2} \end{pmatrix} = \begin{pmatrix} 1/\sqrt{2} & \frac{k_m+im}{E\sqrt{2}} & & \\ 1/\sqrt{2} & -\frac{k_m+im}{E\sqrt{2}} & & \\ & & -1 & \\ & & & 1 \end{pmatrix} \begin{pmatrix} h \\ B_\lambda \\ B_{\tau 1} \\ B_{\tau 2} \end{pmatrix},
\tag{111}
$$

while inverting and substituting $k = +k_m$ gives the equation for particles incident from the unbroken phase:

$$
\begin{pmatrix} h \\ B_\lambda \\ B_{\tau 1} \\ B_{\tau 2} \end{pmatrix} = \begin{pmatrix} 1/\sqrt{2} & 1/\sqrt{2} & & \\ -\frac{k_m+im}{E\sqrt{2}} & \frac{k_m+im}{E\sqrt{2}} & & \\ & & 1 & \\ & & & 1 \end{pmatrix} \begin{pmatrix} \phi^+ \\ \phi^- \\ A_{T1} \\ A_{T2} \end{pmatrix}.
\tag{112}
$$

We attach subscripts to the symbols r, t, R, and T to indicate to which internal mode they apply. As before, the symbols r and t represent reflection and transmission coefficients for a particle incident from $+\infty$, so for example we have

$$
T_\lambda = \frac{k_m}{k_M} |t_\lambda|^2.
\tag{113}
$$

25

Using the method described at the beginning of this section, we calculate the transmission probabilities for a B_L particle incident from the broken phase. We follow the initial amplitude vector through the processes of conversion into internal modes, transmission, and conversion into asymptotic modes at $-\infty$, finding

$$
\begin{pmatrix} 0 \\ 1 \\ 0 \\ 0 \end{pmatrix} \overset{(110)}{\longrightarrow} \begin{pmatrix} 0 \\ -\frac{\omega k_M}{E\sqrt{p^2+k_M^2}} \\ \frac{pM}{E\sqrt{p^2+k_M^2}} \\ 0 \end{pmatrix} \rightarrow \begin{pmatrix} 0 \\ -t_\lambda \frac{\omega k_M}{E\sqrt{p^2+k_M^2}} \\ t_\tau \frac{pM}{E\sqrt{p^2+k_M^2}} \\ 0 \end{pmatrix} \tag{114}
$$

$$
\overset{(111)}{\longrightarrow} \begin{pmatrix} -\frac{k_m+im}{E\sqrt{2}}\, t_\lambda\, \frac{\omega k_M}{E\sqrt{p^2+k_M^2}} \\ \frac{k_m+im}{E\sqrt{2}}\, t_\lambda\, \frac{\omega k_M}{E\sqrt{p^2+k_M^2}} \\ -t_\tau \frac{pM}{E\sqrt{p^2+k_M^2}} \\ 0 \end{pmatrix}.
$$

To obtain transmission probabilities we take the norm of each element of the final vector and multiply each by the appropriate momentum ratio. The resulting transmission probability vector is

$$
\begin{pmatrix} \frac{1}{2}\frac{k_m}{k_M}|t_\lambda|^2\, P \\ \frac{1}{2}\frac{k_m}{k_M}|t_\lambda|^2\, P \\ \frac{k_0}{k_M}|t_\tau|^2\, Q \\ 0 \end{pmatrix} \equiv \begin{pmatrix} \frac{1}{2}PT_\lambda \\ \frac{1}{2}PT_\lambda \\ QT_\tau \\ 0 \end{pmatrix}, \tag{115}
$$

where the probabilities P and Q are

$$
P \;=\; \frac{\omega^2 k_M^2}{E^2(p^2+k_M^2)} \tag{116}
$$

$$
Q = 1 - P \;=\; \frac{p^2 M^2}{E^2(p^2+k_M^2)}. \tag{117}
$$

The normal connection probability P ranges from unity at normal incidence to zero at grazing incidence; its behavior at intermediate angles is shown in figure 4.
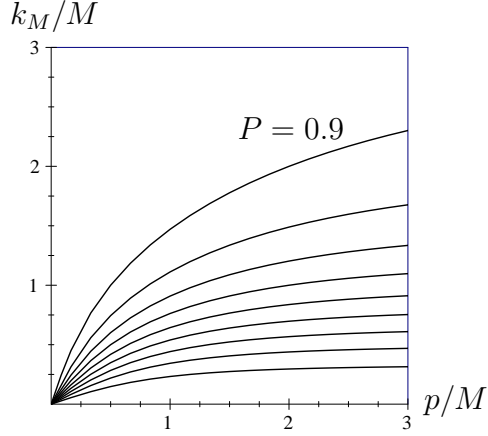
Figure 4: Contour plot of the normal connection probability P as a function of p/M and k_M/M, with contour interval 0.1. The probability P is unity at normal incidence and zero at grazing incidence.

The results (115) of the previous calculation suggest a simpler method which we describe for the case of transmission in the ϕ^+ mode. As indicated in figure 5 there is only one path from B_L to ϕ^+. Since there is no interference between different paths we can calculate with probabilities instead of probability amplitudes and can read off the transmission probability $PT_\lambda/2$ directly. Using this method we obtain most of the scattering probabilities given in table 3. For generality we do not make use of the fact that $T_h \equiv 1$. The only entries of table 3 that require further calculation are the ones that describe reflection of the modes B_L and B_{T1} and reflection of the charged scalars ϕ^+ and ϕ^-.
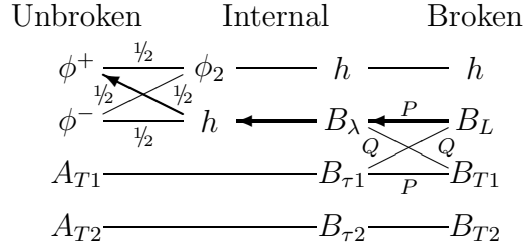
Figure 5: The unique path from B_L to ϕ^+.

	ϕ^+	ϕ^-	A_{T1}	A_{T2}	h	B_L	B_{T1}	B_{T2}
ϕ^+	R_ϕ	X_ϕ			$T_h/2$	$PT_\lambda/2$	$QT_\lambda/2$	
ϕ^-	X_ϕ	R_ϕ			$T_h/2$	$PT_\lambda/2$	$QT_\lambda/2$	
A_{T1}			R_τ			QT_τ	PT_τ	
A_{T2}				R_τ				T_τ
h	$T_h/2$	$T_h/2$			R_h			
B_L	$PT_\lambda/2$	$PT_\lambda/2$	QT_τ			R_L	X	
B_{T1}	$QT_\lambda/2$	$QT_\lambda/2$	PT_τ			X	R_{T1}	
B_{T2}				T_τ				R_τ

Table 3: Scattering probabilities for asymptotic modes. A blank entry indicates a probability of zero.

3.6 Interference between internal modes

We consider the reflection of an incident B_L particle. The amplitude vectors for the process are

$$
\begin{pmatrix} 0 \\ 1 \\ 0 \\ 0 \end{pmatrix} \overset{(110)}{\rightarrow} \begin{pmatrix} 0 \\ -\frac{\omega k_M}{E\sqrt{p^2+k_M^2}} \\ \frac{pM}{E\sqrt{p^2+k_M^2}} \\ 0 \end{pmatrix} \rightarrow \begin{pmatrix} 0 \\ -r_\lambda\,\frac{\omega k_M}{E\sqrt{p^2+k_M^2}} \\ r_\tau\,\frac{pM}{E\sqrt{p^2+k_M^2}} \\ 0 \end{pmatrix} \tag{118}
$$

$$
\overset{(109)}{\rightarrow} \begin{pmatrix} 0 \\ -r_\lambda\,\big(\frac{\omega k_M}{E\sqrt{p^2+k_M^2}}\big)^2 + r_\tau\,\big(\frac{pM}{E\sqrt{p^2+k_M^2}}\big)^2 \\ (r_\lambda + r_\tau)\,\frac{\omega k_M}{E\sqrt{p^2+k_M^2}}\,\frac{pM}{E\sqrt{p^2+k_M^2}} \\ 0 \end{pmatrix}.
$$

We take the norm of the elements of the final amplitude vector to obtain two reflection probabilities, the probability R_L of reflection of B_L as itself and the probability X of crossing, that is, of reflection of B_L into B_{T1}. When we calculate the corresponding reflection probabilities for a B_{T1} particle, we find that the crossing probability X also describes reflection of B_{T1} into B_L. The reflection probabilities are

$$
\begin{aligned}
R_L &= P^2 R_\lambda + Q^2 R_\tau - 2PQ\sqrt{R_\lambda R_\tau}\,\chi & (119) \\
R_{T1} &= Q^2 R_\lambda + P^2 R_\tau - 2PQ\sqrt{R_\lambda R_\tau}\,\chi & (120) \\
X &= PQ\,R_\lambda + PQ\,R_\tau + 2PQ\sqrt{R_\lambda R_\tau}\,\chi, & (121)
\end{aligned}
$$

where the crossing enhancement factor χ is defined by

$$
\chi = \mathrm{Re}\Big[\frac{r_\lambda^* r_\tau}{|r_\lambda||r_\tau|}\Big]. \tag{122}
$$

The interference term which appears in equations (119)–(121) is proportional to the factor χ, the cosine of the angle between the amplitudes r_λ and r_τ. When χ is positive, the interference term increases the probability of crossing. For mass ratios $\mathcal{M}^2 > 1$ the behavior of χ as a function
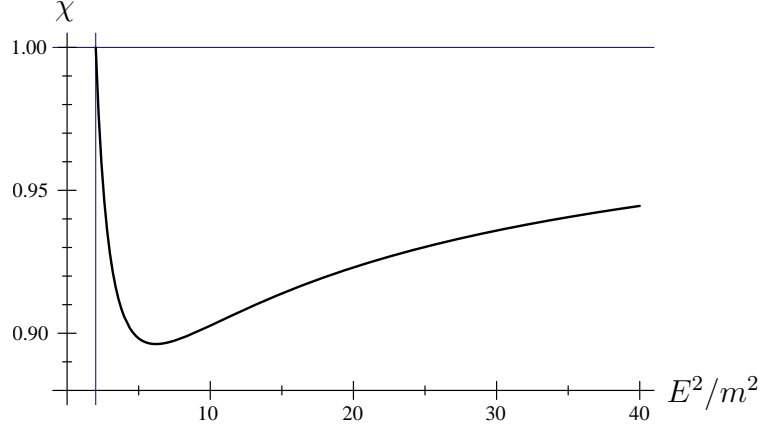
Figure 6: Crossing enhancement factor χ as a function of E^2/m^2 for a mass ratio $\mathcal{M}^2$ of 2.

of E^2/m^2 is not complicated. The curve shown in figure 6 is typical—χ drops from the value 1 at the threshold $E^2/m^2 = \mathcal{M}^2$ to a positive minimum, then returns gradually to 1.

We plot a set of representative curves for mass ratios $\mathcal{M}^2 < 1$ in figure 7. In the region $E^2/m^2 > 1$ the curves all exhibit the same positive minimum and gradual return to 1, but in the region $E^2/m^2 < 1$ where the B_λ mode is totally reflected, the curves are qualitatively different from one another. The mass ratio $\mathcal{M}^2$ at which the cusp at $E^2/m^2 = 1$ reaches unit height is only approximately 0.4225, but the ratio at which the $\chi = -1$ minimum vanishes is *exactly* 3/4, the same ratio at which the bound state in the B_λ mode appears.

Analogous calculations for the reflection of the charged scalars ϕ^+ and ϕ^- yield the reflection probabilities

$$R_\phi = \tfrac{1}{4}\left(R_h + R_\lambda - 2\sqrt{R_h R_\lambda}\,\chi_\phi\right) \tag{123}$$

$$X_\phi = \tfrac{1}{4}\left(R_h + R_\lambda + 2\sqrt{R_h R_\lambda}\,\chi_\phi\right) \tag{124}$$

where

$$\chi_\phi = \mathrm{Re}\left[\left(\frac{k_m + im}{E}\right)^2 \frac{r_h^* r_\lambda}{|r_h||r_\lambda|}\right]. \tag{125}$$
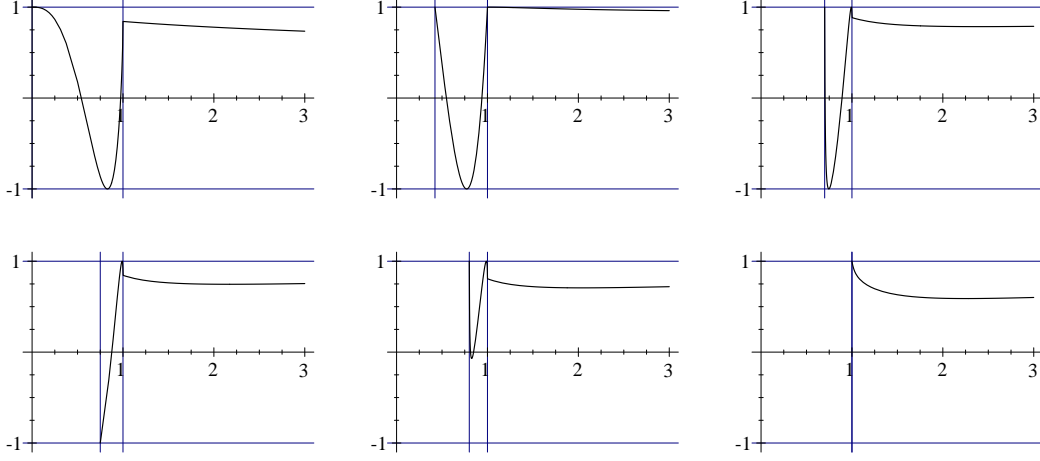
30

Figure 7: Crossing enhancement factor χ as a function of E^2/m^2 for gauge boson mass ratios $\mathcal{M}^2$ of 0, 0.4225, 0.7, 3/4, 0.8, and 1.

For the quartic Higgs potential (75) these results for charged scalars simplify—the amplitude r_h is identically zero, χ_ϕ is undefined, and the reflection probabilities R_ϕ and X_ϕ both reduce to $R_\lambda/4$.

3.7 Discussion of results

For particles with energy sufficiently far above all relevant mass thresholds the internal mode transmission probabilities are essentially unity and the process of scattering from the domain wall can be regarded as a process of conversion of particles between phases. In this limit the scattering probabilities in table 3 reduce to the conversion probabilities in table 4. The breakdown of this approximation occurs when either the momentum of the incident particle approaches zero or one of the internal modes to which the particle connects approaches total reflection.

We consider the extent to which our results based on the quartic potential of equation (75) apply when the Higgs potential is more general. With the exception of the plots of χ, the results of sections 3.5 and 3.6 hold for

	h	B_L	B_{T1}	B_{T2}
ϕ^+	1/2	$P/2$	$Q/2$	
ϕ^-	1/2	$P/2$	$Q/2$	
A_{T1}		Q	P	
A_{T2}				1

Table 4: Conversion probabilities for high-energy particles.

an arbitrary Higgs potential—all dependence on the potential is contained in the reflection and transmission amplitudes for the internal modes. From the discussion of bound states in section 3.3 we draw the following generally applicable conclusions: The potential U_τ is always monotone increasing, so the B_τ modes never have bound states. The B_λ mode need not have a bound state, but is capable of supporting at least one. The h mode is guaranteed to have at least one bound state. We cannot make any more specific statement about the bound states of the h mode, because for any positive integer there exist Higgs potentials $V(v)$ for which the h mode has that number of bound states. Suitable Higgs potentials can be constructed by joining three quadratic pieces; the resulting scattering potentials $U_h = V''(v)$ are square wells of various sizes.

4 Extension to the standard model

4.1 Reduction to two subproblems

The fields appearing in the standard model are listed in table 5, along with their transformation properties under the various symmetry groups. We take the symbols B^μ and, later, A^μ to have completely different meanings than in the previous sections.

	Spin	Family	Y	$SU(2)$	$SU(3)$
B^μ	1	-	0	-	-
W^μ	1	-	0	triplet	-
G^μ	1	-	0	-	octet
ϕ	0	-	$+1$	$\checkmark$	-
ℓ_L	1/2	$\checkmark$	-1	$\checkmark$	-
e_R	1/2	$\checkmark$	-2	-	-
q_L	1/2	$\checkmark$	$1/3$	$\checkmark$	$\checkmark$
u_R	1/2	$\checkmark$	$4/3$	-	$\checkmark$
d_R	1/2	$\checkmark$	$-2/3$	-	$\checkmark$

Table 5: Fields appearing in the standard model. A check indicates that the field transforms according to the fundamental representation of the corresponding group.

The standard model Lagrangian is

$$
\begin{aligned}
\mathcal{L} \;=\; & -\; \frac{1}{4} B_{\mu\nu} B^{\mu\nu} - \frac{1}{4} W^i_{\mu\nu} W^{i\,\mu\nu} - \frac{1}{4} G^a_{\mu\nu} G^{a\,\mu\nu} \\
& +\; (D_\mu \phi)^\dagger (D^\mu \phi) - V(\sqrt{2}\,|\phi|) \\
& + \Big(\frac{i}{2} \bar{\ell}_L \slashed{D} \ell_L + \frac{i}{2} \bar{e}_R \slashed{D} e_R + \frac{i}{2} \bar{q}_L \slashed{D} q_L + \frac{i}{2} \bar{u}_R \slashed{D} u_R + \frac{i}{2} \bar{d}_R \slashed{D} d_R \\
& \qquad\qquad - \bar{\ell}_L M_e \phi\, e_R - \bar{q}_L M_u \phi_c u_R - \bar{q}_L M_d \phi\, d_R \;+\; \text{H. c.} \Big).
\end{aligned}
\tag{126}
$$

For equation (126) we define the norm $|\phi|$ by

$$
|\phi| = \sqrt{\phi^\dagger \phi}
\tag{127}
$$

and the conjugate field ϕ_c by

$$
\phi_c = i\tau_2 \phi^*.
\tag{128}
$$

The constants M_e, M_u, and M_d are matrices in family space.

To study scattering from a domain wall at the electroweak phase transition, we will write out the components of ϕ,

$$
\phi = \frac{1}{\sqrt{2}} \begin{pmatrix} \phi_3 + i\phi_4 \\ \phi_1 + i\phi_2 \end{pmatrix},
\tag{129}
$$

33

derive equations of motion, define

$$\phi_1 = v + h, \tag{8}$$

take all fields except v to be perturbatively small, and obtain an equation for the static domain wall solution v along with first-order equations of motion which describe perturbations about it. First, however, we simplify the calculation by removing from the Lagrangian terms which do not contribute to the end result, such as terms higher than quadratic in fields other than ϕ.

Specifically, we remove the bilinear terms from the gauge field strengths and the gauge couplings from the fermion covariant derivatives. The fermion mass terms are quadratic in the perturbatively small fermion fields and so do not contribute to the equations of motion for ϕ. Consequently, we can expand ϕ according to equations (129) and (8) even before deriving the equations of motion. Dropping higher than quadratic terms yields the simplified mass terms

$$\left(-\bar{e}_L \frac{vM_e}{\sqrt{2}} e_R - \bar{u}_L \frac{vM_u}{\sqrt{2}} u_R - \bar{d}_L \frac{vM_d}{\sqrt{2}} d_R \ + \ \text{H. c.} \right). \tag{130}$$

Redefining the fermion fields by applying independent unitary rotations in family space to the left and right components of the fields e, u, and d allows us to take the mass matrices M_e, M_u, and M_d to be diagonal with positive real eigenvalues.

As a result of the above transformations the Lagrangian (126) falls into unrelated pieces. For each massive fermion species there is a copy of the Dirac Lagrangian

$$\left(\frac{i}{2} \bar{\psi} \slashed{\partial} \psi \ + \ \text{H. c.} \right) - (\mu v) \bar{\psi} \psi \tag{131}$$

with a broken-phase mass μv_0 equal to $v_0 / \sqrt{2}$ times the eigenvalue of the appropriate mass matrix. We consider the massive fermions further in section 4.3. The pieces of the Lagrangian which describe neutrinos

$$\left(\frac{i}{2} \bar{\nu}_L \slashed{\partial} \nu_L \ + \ \text{H. c.} \right) \tag{132}$$

34

and gluons

$$-\frac{1}{4}(\partial_\mu G_\nu^a - \partial_\nu G_\mu^a)(\partial^\mu G^{a\,\nu} - \partial^\nu G^{a\,\mu}) \tag{133}$$

are Lagrangians of free particles. To first order the neutrinos and gluons do not interact with the domain wall, and we do not consider them further. The remainder of the original Lagrangian,

$$-\frac{1}{4}B_{\mu\nu}B^{\mu\nu} \quad - \quad \frac{1}{4}(\partial_\mu W_\nu^i - \partial_\nu W_\mu^i)(\partial^\mu W^{i\nu} - \partial^\nu W^{i\mu})$$
$$+ \quad (D_\mu \phi)^\dagger (D^\mu \phi) - V(\sqrt{2}\,|\phi|), \tag{134}$$

we analyze in the following section.

4.2   Standard model bosons

Having reduced the standard model Lagrangian (126) to the boson Lagrangian (134), we apply the method described in the previous section and derive equations of motion. After some calculation, we find that the condition for the field configuration $v(z)$ to be stable

$$v'' = V'(v) \tag{9}$$

and the first-order equation of motion for the field h

$$\Box h = -V''(v)h \tag{11}$$

are the same as in the Abelian Higgs model. The equations of motion for the fields ϕ_3 and $W^{2\,\mu}$,

$$\Box \phi_3 \quad = \quad -\tfrac{1}{2}gv\,\partial \cdot W^2 - gW^{2\mu}\partial_\mu v - \frac{V'(v)}{v}\phi_3 \tag{135}$$
$$\partial_\nu \widetilde{W}^{2\,\mu\nu} \quad = \quad \tfrac{1}{2}g(v\partial^\mu \phi_3 - \phi_3 \partial^\mu v) + (\tfrac{1}{2}gv)^2 W^{2\,\mu}, \tag{136}$$

where

$$\widetilde{W}^{i\,\mu\nu} = \partial^\mu W^{i\nu} - \partial^\nu W^{i\mu}, \tag{137}$$

are exact analogues of equations (12) and (13) for ϕ_2 and A^μ, as are the equations of motion for ϕ_4 and $W^{1\,\mu}$:

$$\Box\phi_4 \;=\; -\tfrac{1}{2}gv\,\partial\cdot W^1 - gW^{1\mu}\partial_\mu v - \frac{V'(v)}{v}\phi_4 \tag{138}$$

$$\partial_\nu \widetilde{W}^{1\,\mu\nu} \;=\; \tfrac{1}{2}g(v\partial^\mu\phi_4 - \phi_4\partial^\mu v) + (\tfrac{1}{2}gv)^2 W^{1\,\mu}. \tag{139}$$

To cast the last three equations of motion

$$\Box\phi_2 \;=\; -\tfrac{1}{2}v\,\partial\cdot(g'B - gW^3) - (g'B^\mu - gW^{3\mu})\partial_\mu v - \frac{V'(v)}{v}\phi_2 \tag{140}$$

$$\partial_\nu \widetilde{W}^{3\,\mu\nu} \;=\; -\tfrac{1}{2}g\,(v\partial^\mu\phi_2 - \phi_2\partial^\mu v) - \tfrac{1}{4}g\,v^2(g'B^\mu - gW^{3\mu}) \tag{141}$$

$$\partial_\nu B^{\mu\nu} \;=\; \tfrac{1}{2}g'(v\partial^\mu\phi_2 - \phi_2\partial^\mu v) + \tfrac{1}{4}g'v^2(g'B^\mu - gW^{3\mu}) \tag{142}$$

into a form analogous to equations (12) and (13), we define the linear combinations

$$Z^\mu = \frac{g'B^\mu - gW^{3\mu}}{\sqrt{g^2 + g'^2}} \qquad \text{and} \qquad A^\mu = \frac{gB^\mu + g'W^{3\mu}}{\sqrt{g^2 + g'^2}} \tag{143}$$

and obtain equations of motion for ϕ_2 and Z^μ

$$\Box\phi_2 \;=\; -\tfrac{1}{2}\sqrt{g^2 + g'^2}\, v\,\partial\cdot Z - \sqrt{g^2 + g'^2}\, Z^\mu\partial_\mu v - \frac{V'(v)}{v}\phi_2 \tag{144}$$

$$\partial_\nu Z^{\mu\nu} \;=\; \tfrac{1}{2}\sqrt{g^2 + g'^2}\,(v\partial^\mu\phi_2 - \phi_2\partial^\mu v) + (\tfrac{1}{2}\sqrt{g^2 + g'^2}\, v)^2\, Z^\mu \tag{145}$$

along with an equation of motion

$$\partial_\nu F^{\mu\nu} = 0 \tag{146}$$

which describes a noninteracting massless gauge boson—the photon.

We summarize the correspondence between the standard model and the Abelian Higgs model in the following table.

A^μ	ϕ_2	e	B^μ	M
$W^{1\,\mu}$	ϕ_4	$\tfrac{1}{2}g$	$\mathcal{W}^{1\,\mu}$	M_W
$W^{2\,\mu}$	ϕ_3	$\tfrac{1}{2}g$	$\mathcal{W}^{2\,\mu}$	M_W
Z^μ	ϕ_2	$\tfrac{1}{2}\sqrt{g^2 + g'^2}$	$\mathcal{Z}^\mu$	M_Z

$$\tag{147}$$

The right side of the table shows the names we assign to the analogues of B^μ and M. From the defining equations (28) and (30) for B^μ and M we find, for example,

$$\mathcal{W}^{2\mu} = W^{2\mu} + \partial^\mu \left(\frac{\phi_3}{\frac{1}{2}gv} \right) \tag{148}$$

$$M_W^2 = (\tfrac{1}{2}gv_0)^2. \tag{149}$$

By applying the above correspondence to our results for the Abelian Higgs model we can find out nearly everything we want to know about standard model bosons. To be specific, we obtain the definitions and scattering potentials of the scalar internal modes and most of the equations that connect the internal modes to the asymptotic ones. What the correspondence fails to provide is the connection between the real Higgs modes h, ϕ_2, ϕ_3 and ϕ_4 and the complex modes appropriate to the unbroken phase. The modes h and ϕ_2 combine just as in the Abelian Higgs model—copying equation (73) we define the amplitudes of the particle and antiparticle solutions

$$\phi^0 = \frac{h + i\phi_2}{\sqrt{2}} \qquad \text{and} \qquad \bar{\phi}^0 = \frac{h - i\phi_2}{\sqrt{2}} \tag{150}$$

and obtain the connection diagram given in figure 8. The associated connection equations, scattering probabilities, and conversion probabilities may be found by applying the correspondence to equations (55) and (74) and tables 3 and 4.

Since the Higgs fields ϕ_3 and ϕ_4 combine with each other rather than with the field h in the charged particle and antiparticle amplitudes

$$\phi^+ = \frac{\phi_3 + i\phi_4}{\sqrt{2}} \qquad \text{and} \qquad \phi^- = \frac{\phi_3 - i\phi_4}{\sqrt{2}}, \tag{151}$$

the connection equations involving these modes will not be exact analogues of the connection equations of the Abelian Higgs model. Taking the relevant parts of equations (55) and (74) and applying the correspondence, we obtain
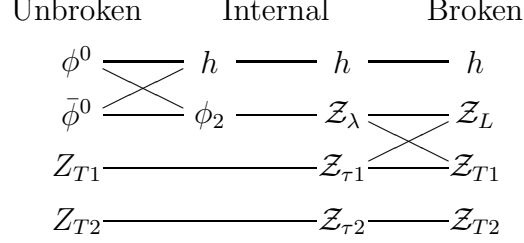
37

Figure 8: Connections between neutral modes in the standard model.

the reduced connection equations

$$
\begin{pmatrix} \phi_3 \\ W_{T1}^2 \\ W_{T2}^2 \end{pmatrix} = \begin{pmatrix} \frac{m+ik}{E} & & \\ & \operatorname{sgn} k & \\ & & 1 \end{pmatrix} \begin{pmatrix} \mathcal{W}_\lambda^2 \\ \mathcal{W}_{\tau 1}^2 \\ \mathcal{W}_{\tau 2}^2 \end{pmatrix}
\tag{152}
$$

and

$$
\begin{pmatrix} \mathcal{W}_L^2 \\ \mathcal{W}_{T1}^2 \\ \mathcal{W}_{T2}^2 \end{pmatrix} = \begin{pmatrix} \frac{\omega k}{E\sqrt{p^2+k^2}} & \frac{pM}{E\sqrt{p^2+k^2}} & \\ -\frac{pM}{E\sqrt{p^2+k^2}} & \frac{\omega k}{E\sqrt{p^2+k^2}} & \\ & & 1 \end{pmatrix} \begin{pmatrix} \mathcal{W}_\lambda^2 \\ \mathcal{W}_{\tau 1}^2 \\ \mathcal{W}_{\tau 2}^2 \end{pmatrix}
\tag{153}
$$

along with a similar pair for the fields W^1 and ϕ_4. We define charged gauge boson amplitudes for each of the internal and asymptotic gauge boson modes, for example,

$$
W_{T1}^+ = \frac{W_{T1}^2 + iW_{T1}^1}{\sqrt{2}} \qquad \text{and} \qquad W_{T1}^- = \frac{W_{T1}^2 - iW_{T1}^1}{\sqrt{2}}.
\tag{154}
$$

Since the definitions (151) and (154) describe the same linear transformation of amplitudes, the connection matrices for the charged bosons are identical to those in equations (152) and (153). We present one of the associated connection diagrams in figure 9; the absence of connections between positive and negative bosons is of course guaranteed by the conservation of electric charge.[4] Applying the methods of sections 3.5 and 3.6 produces the scattering

---

[4]The correct analogue of the charge non-conservation in scattering in the Abelian Higgs model is the non-conservation of isospin and hypercharge, for example, in the reflection process $\phi^0 \rightarrow \bar{\phi}^0$.
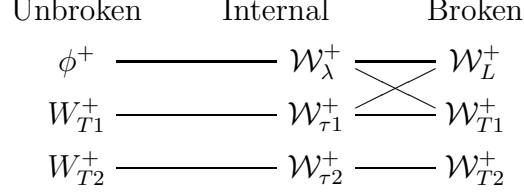
Unbroken   Internal   Broken

$$\phi^+ \text{————} \mathcal{W}_\lambda^+ \diagdown\diagup \mathcal{W}_L^+$$
$$W_{T1}^+ \text{————} \mathcal{W}_{\tau 1}^+ \diagup\diagdown \mathcal{W}_{T1}^+$$
$$W_{T2}^+ \text{————} \mathcal{W}_{\tau 2}^+ \text{————} \mathcal{W}_{T2}^+$$

Figure 9: Connections between charged modes in the standard model.

	ϕ^+	W_{T1}^+	W_{T2}^+	$\mathcal{W}_L^+$	$\mathcal{W}_{T1}^+$	$\mathcal{W}_{T2}^+$
ϕ^+	R_λ			PT_λ	QT_λ	
W_{T1}^+		R_τ		QT_τ	PT_τ	
W_{T2}^+			R_τ			T_τ
$\mathcal{W}_L^+$	PT_λ	QT_τ		R_L	X	
$\mathcal{W}_{T1}^+$	QT_λ	PT_τ		X	R_{T1}	
$\mathcal{W}_{T2}^+$			T_τ			R_τ

Table 6: Scattering probabilities for charged modes in the standard model.

probabilities given in table 6 and the conversion probabilities, that is, the transmission probabilities for high-energy particles, given in table 7.

4.3   Scattering of fermions

Variation of the Dirac Lagrangian (131) gives the Dirac equation

$$(i\slashed{\partial} - \mu v)\psi = 0. \tag{155}$$

	$\mathcal{W}_L^+$	$\mathcal{W}_{T1}^+$	$\mathcal{W}_{T2}^+$
ϕ^+	P	Q	
W_{T1}^+	Q	P	
W_{T2}^+			1

Table 7: Conversion probabilities for charged modes in the standard model.

To reduce this equation to scattering equations for scalar internal modes we use the ansatz of Ayala et al [2]

$$\psi = (i\slashed{\partial} + \mu v)\tilde{\psi} \tag{156}$$

to obtain

$$\left[\Box + (\mu v)^2 - i\gamma^3(\mu v')\right]\tilde{\psi} = 0. \tag{157}$$

We take $\tilde{\psi}$ to be proportional to an eigenvector $u_\pm$ of the matrix $-i\gamma^3$ with eigenvalue ± 1,

$$\tilde{\psi} = u_\pm f_\pm, \tag{158}$$

and find that the corresponding scalar function $f_\pm$ satisfies the scattering equation

$$\left[\Box + U_{f\pm}(z)\right] f_\pm = 0 \tag{159}$$

with potential

$$U_{f\pm} = (\mu v)^2 \pm \mu v'. \tag{160}$$

The existence of two different potentials for fermion scattering is an artifact of the process of extracting scalar modes, because any solution ψ of equation (155) can be expressed in terms of either f_+ or f_-. For example, the solution ψ generated by an eigenvector u_- and function f_- can also be obtained from the eigenvector u_+ and function f_+ given by

$$u_+ = \frac{1}{E}\left(\sum_{\mu \neq 3} \gamma^\mu p_\mu\right) u_- \tag{161}$$

$$f_+ = \frac{1}{E}\left(\mu v + \partial_3\right) f_-. \tag{162}$$

We will express our results in terms of u_+ and f_+, because of the following advantage of the potential U_{f+}: being the sum of two positive terms which go to zero at $-\infty$, it has no absolute minimum and so clearly has no bound states.

Although we have reduced the Dirac equation (155) to a scalar equation (159), we have not yet defined internal and asymptotic modes for the fermion field. For the moment we consider only positive-energy solutions of equation (155). In the Pauli-Dirac representation of the matrices γ^μ, the normalized asymptotic solutions for the field ψ can be written in terms of a two-component spinor φ as

$$\psi[\varphi] = \frac{1}{2\sqrt{\omega + \mu v}} \begin{pmatrix} \omega + \mu v \\ \vec{p} \cdot \vec{\sigma} \end{pmatrix} \varphi \, \mathrm{e}^{-ip \cdot x}. \tag{163}$$

Our normalization—setting the z-component of energy flux equal to $\frac{1}{2}\omega k$— is compatible with massless particles, so these asymptotic solutions can be used in both the broken and unbroken phases. The two-component spinor φ describes the spin of the fermion in its rest frame; our normalization assumes it satisfies

$$\varphi^\dagger \varphi = 1. \tag{164}$$

To study the relation between internal and asymptotic solutions we consider a solution f_+ which is asymptotically a unit-amplitude plane wave:

$$f_+ = \mathrm{e}^{-ip \cdot x}. \tag{165}$$

We write the eigenvector u_+ in the form

$$u_+ = (1 - i\gamma^3) \begin{pmatrix} \chi \\ 0 \end{pmatrix}, \tag{166}$$

where χ is a constant two-component spinor. Substituting into the definitions (156) and (158), we find that the resulting asymptotic field ψ is equal to $\psi[\varphi]$ for the following unnormalized spinor φ:

$$\varphi = \frac{2}{\sqrt{\omega + \mu v}} \begin{pmatrix} \omega + \mu v - ik & ip \\ -ip & \omega + \mu v - ik \end{pmatrix} \chi. \tag{167}$$

As before, we choose the coordinate system so that the transverse momentum p lies along the x-axis. Because the values of the quantities k and v

41

appearing in equation (167) depend on whether the particle is in the broken or unbroken phase and on what the sign of the z-momentum is, the spin direction determined by φ can change as a result of the scattering process. However, the particular choices

$$\chi = \begin{pmatrix} 1 \\ \pm i \end{pmatrix} \tag{168}$$

generate spinors

$$\varphi = \frac{2}{\sqrt{\omega + \mu v}}(\omega + \mu v \mp p - ik)\,\chi \tag{169}$$

which point in the directions $\hat{y}$ and $-\hat{y}$ independent of the values of k and v. Accordingly, we define the internal modes $f_{+\uparrow}$ and $f_{+\downarrow}$ to have spins aligned with the y-axis, that is, to have the normalized polarization spinors

$$\chi_\uparrow = \frac{1}{2\sqrt{2(\omega - p)}}\,\frac{1}{\sqrt{2}}\begin{pmatrix} 1 \\ i \end{pmatrix} \qquad \text{and} \qquad \chi_\downarrow = \frac{1}{2\sqrt{2(\omega + p)}}\,\frac{1}{\sqrt{2}}\begin{pmatrix} 1 \\ -i \end{pmatrix}. \tag{170}$$

Although equation (169) contains the nonconstant quantities k and v, the normalized spinors $\chi_\uparrow$ and $\chi_\downarrow$ are constant, as required, as a result of the identity

$$|\omega + \mu v \mp p - ik|^2 = 2(\omega + \mu v)(\omega \mp p). \tag{171}$$

Defining the asymptotic modes

$$\psi_\uparrow = \psi\left[\frac{1}{\sqrt{2}}\begin{pmatrix} 1 \\ i \end{pmatrix}\right] \qquad \text{and} \qquad \psi_\downarrow = \psi\left[\frac{1}{\sqrt{2}}\begin{pmatrix} 1 \\ -i \end{pmatrix}\right] \tag{172}$$

we obtain the connection equation

$$\begin{pmatrix} \psi_\uparrow \\ \psi_\downarrow \end{pmatrix} = \begin{pmatrix} \frac{\omega + \mu v - p - ik}{\sqrt{(\omega + \mu v - p)^2 + k^2}} & \\ & \frac{\omega + \mu v + p - ik}{\sqrt{(\omega + \mu v + p)^2 + k^2}} \end{pmatrix} \begin{pmatrix} f_{+\uparrow} \\ f_{+\downarrow} \end{pmatrix} \tag{173}$$

which is valid in both the broken and unbroken phases when the appropriate values of k and v are used. Because the connection matrix is diagonal, we

conclude that our chosen asymptotic modes do not interconnect and that the scattering probabilities for each of the asymptotic modes are equal to the scattering probabilities R_{f+} and T_{f+} for the internal mode f_+. The appearance of nontrivial complex phases in the connection matrix of equation (173) indicates that in general the spin of the fermion rotates about the y-axis during scattering.

To obtain the negative-energy solutions of the Dirac equation (155) we make use of the charge conjugation symmetry[5]

$$\psi \to i\gamma^2 \psi^*. \tag{174}$$

Applying charge conjugation to an incident negative-energy particle produces an incident positive-energy particle, for which we know the solution of equation (155). Applying charge conjugation again yields the desired negative-energy solution. Under charge conjugation the magnitudes of the coefficients of the scattered waves do not change, so the negative-energy solutions have the same reflection and transmission probabilities R_{f+} and T_{f+} as the positive-energy solutions.

For the quartic Higgs potential (75), the scattering potential U_{f+} can be written in the standard form (78), so we can obtain the reflection and transmission probabilities R_{f+} and T_{f+} from equations (104) and (105). For reference, the coefficients of the potential U_{f+} are

$$U_0 = 0 \tag{175}$$
$$U_1 = \mathcal{M}_f^2 \tag{176}$$
$$U_2 = \mathcal{M}_f(1 - \mathcal{M}_f), \tag{177}$$

where the mass ratio $\mathcal{M}_f^2$ is defined to be $(\mu v_0)^2/m^2$. The scattering probabilities so obtained agree with those of Ayala et al [2]. Our discussion of

---

[5]We do not simply take ω to be negative, because the analysis of asymptotic behavior in section 3.2 relies on the positive energy of the solution.
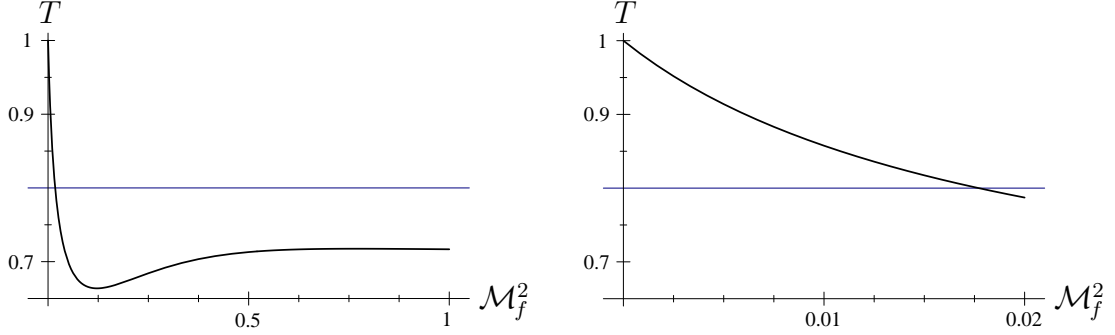
Figure 10: Transmission probability near threshold for the f_+ mode, plotted as a function of $\mathcal{M}_f^2$. The energy E^2 is taken to be $(\mu v_0)^2 + 0.01\,m^2$.

fermion scattering differs from theirs primarily in that we have explicitly considered the polarization of the fermion.

According to the results of section 3.4 the transmission probability as a function of E^2/m^2 has the generic form described in that section unless the scattering potential is close to a potential which gives $T \equiv 1$, in which case the onset of transmission is more abrupt. Just such an increasing abruptness of onset occurs in the f_+ mode as the mass ratio $\mathcal{M}_f^2$ goes to zero. The effect can be seen in figure 10, in which we plot the transmission probability at a fixed distance above the threshold of total reflection as a function of the mass ratio $\mathcal{M}_f^2$. Although the same effect occurs within the B_τ mode, it is of less practical importance in that case, because the gauge boson masses M_W and M_Z are of the same order of magnitude as the Higgs mass m, while the fermion masses are generally much smaller.

5 Conclusion

We have resolved the difficulties associated with the change of particle content across a domain wall at a symmetry-breaking phase transition and obtained scattering solutions for scalar and gauge bosons. The relationship between the modes ϕ_2 and B_λ provides a precise statement of the intuition

that in a spontaneously broken gauge theory each apparent Goldstone boson turns into the longitudinal polarization of a massive gauge boson.

Our results should prove fundamental to many different calculations involving the electroweak phase transition in the standard model. Although the scattering probabilities for asymptotic particles interacting with a domain wall are interesting for some purposes, we expect that the scalar internal modes, which are capable of describing the gradual change in particle content across a domain wall, will prove a more useful tool in actual calculations.

Note added: We thank M. Voloshin for bringing to our attention earlier related work on this subject, in which the spontaneous breaking of a discrete symmetry was studied using a quartic potential. The single bosonic mode present in that situation obeys the same equations as our h mode. Polyakov [4] found the masses of the bound states of this mode. Voloshin [5] obtained the scattering equation and hypergeometric solutions for this mode, including the bound-state wavefunctions, and observed that the transmission probability is identically one. In the latter work the scattering of fermions axially coupled to the scalar field was also studied.

References

[1] G. R. Farrar and M. E. Shaposhnikov, hep-ph/9305275, Phys. Rev. D **50**, 774 (1994).

[2] A. Ayala, J. Jalilian-Marian, L. McLerran, and A. P. Vischer, hep-ph/9311296, Phys. Rev. D **49**, 5559 (1994). For purposes of comparison we mention that as a result of the quartic nature of the Higgs potential V, their parameter ξ, defined to be *twice* the ratio of fermion to Higgs mass at *zero* temperature, is exactly equal to our mass ratio $\mathcal{M}_f$.

[3] L. D. Landau and E. M. Lifshitz, *Quantum Mechanics* (Pergamon Press, 1958). The hypergeometric equation is discussed in appendix §e. Exam-

ples of its use appear in the problems in the sections on the linear oscillator (§21) and the transmission coefficient (§23).

[4] A. M. Polyakov, Pis'ma Zh. Eksp. Teor. Fiz. **20**, 430 (1974) [JETP Lett. **20**, 194 (1974)].

[5] M. B. Voloshin, Yad. Fiz. **21**, 1331 (1975) [Sov. J. Nucl. Phys. **21**, 687 (1975)].